



ORIGINAL ARTICLE

## Integrated Bioinformatic and Experimental Analysis of LINC00472, LINC02381, FHIT, and hsa-miR-7-5p Expression, Alongside FHIT Protein, in Esophageal Cancer

Shayan Marhamati<sup>1,2</sup> , Zeinab Seyedkhan<sup>1,2</sup> , Nasrin Ziamajidi<sup>1,3</sup> , Fatemeh Bahreini<sup>4</sup> , Amirnader Emami Razavi<sup>5</sup> , Mahdi Bahmani<sup>1\*</sup> , Roghayeh Abbasalipourkabir<sup>1\*\*</sup>

1. Department of Clinical Biochemistry, Faculty of Medicine, Hamadan University of Medical Sciences, Hamadan, Iran.
2. Student Research Committee, Hamadan University of Medical Sciences, Hamadan, Iran.
3. Research Center for Molecular Medicine, Institute of Cancer, Avicenna Health Research Institute, Hamadan University of Medical Sciences, Hamadan, Iran.
4. Department of Medical Genetics, Faculty of Medicine, Hamadan University of Medical Sciences, Hamadan, Iran.
5. Iran National Tumor Bank, Cancer Institute of Iran, Tehran University of Medical Sciences, Tehran, Iran.

### ARTICLE INFO

**Received:** 2025/10/5  
**Revised:** 2026/01/7  
**Accepted:** 2026/02/2

### ABSTRACT

Esophageal cancer (EC) ranks among the eight most common malignancies worldwide. Long noncoding RNAs LINC00472 and LINC02381 are implicated in cancers, but their role in EC remains unclear. Therefore, this study investigates the roles of LINC00472 and LINC02381 in EC. This study analyzed lncRNA, miRNA, and mRNA sequencing related to EC using TCGA. Then, the LINC00472, LINC02381, hsa-miR-7-5p, and FHIT genes were identified. Expression levels of these genes were assessed in 20 EC tissue pairs using RT- qPCR, while FHIT protein expression was examined by Western blot and Immunohistochemistry. Chi-square tests explored clinicopathological correlations, while ROC analysis evaluated their diagnostic potential. Bioinformatic analysis and RT-qPCR results demonstrated significantly decreased expression of LINC00472, LINC02381, and FHIT ( $p < 0.01$ ), alongside increased hsa-miR-7-5p expression in EC ( $p < 0.0001$ ). A significant reduction in FHIT protein expression was also observed ( $p < 0.01$ ). Correlations showed that LINC02381 and FHIT expressions were positively correlated, while LINC00472 and LINC02381 were negatively associated with hsa-miR-7-5p ( $p < 0.05$ ). Elevated levels of hsa-miR-7-5p were significantly linked to vascular invasion and deeper muscularis propria infiltration in EC ( $p < 0.05$ ). Higher FHIT levels were also linked to increased necrosis and decreased vascular invasion ( $p < 0.05$ ). The ROC analysis demonstrated measurable AUC values for each of the examined genes, suggesting potential diagnostic relevance that warrants further validation. This research revealed dysregulated genes LINC00472, LINC02381, hsa-miR-7-5p, and FHIT in EC, proposing a regulatory network through bioinformatic analyses and correlations. Results establish groundwork for functional studies, emphasizing their potential significance in understanding and controlling EC pathogenesis.

**Keywords:** Esophageal Neoplasm, LINC00472, LINC02381, hsa-miR-7-5p, FHIT, Diagnosis

#### \*Corresponding:

Mahdi Bahmani  
**Address:**  
Department of Clinical Biochemistry, Faculty of Medicine, Hamadan University of Medical Sciences, 6517619657, Hamadan, Iran.  
**E-mail:**  
M.bahmani@umsh.ac.ir;  
bahmani.m64@gmail.com

#### \*Co-corresponding:

Roghayeh Abbasalipourkabir  
**Address:**  
Department of Clinical Biochemistry, Faculty of Medicine, Hamadan University of Medical Sciences, 6517619657, Hamadan, Iran.  
**E-mail:**  
rpourkabir@hotmail.com

**Cite this article:** Marhamati S, et al. Integrated Bioinformatic and Experimental Analysis of LINC00472, LINC02381, FHIT, and hsa-miR-7-5p Expression, Alongside FHIT Protein, in Esophageal Cancer. International Journal of Molecular and Cellular Medicine. 2026; 15 (1):1143-1157. DOI: 10.22088/IJMCM.BUMS.15.1.1143



## Introduction

Esophageal cancer is the eighth most commonly diagnosed cancer worldwide and the sixth most frequent cause of cancer-related deaths. South and South-Central Asia exhibit the highest rates of both incidence and mortality associated with EC (1, 2). Over 95% of individuals with EC receive their diagnosis at a late stage (3). Consequently, gaining deeper insights into the molecular pathways underlying EC may enhance prognostic accuracy and facilitate earlier detection.

Noncoding RNAs constitute a large class of transcripts that, despite lacking protein-coding capacity, play critical roles in regulating gene expression and mRNA translation (4, 5). Some of the ncRNAs that have been identified include long noncoding RNAs (lncRNAs), circular RNAs, and microRNAs (miRNAs) (6). Noncoding RNAs have emerged as key molecular players in cancer biology, functioning either as oncogenic drivers or tumor suppressors in malignancies such as breast cancer, lung cancer, and hepatocellular carcinoma (7).

lncRNAs, which are RNA transcripts over 200 nucleotides in length, contribute to various cellular mechanisms and regulatory pathways (8). According to the competing endogenous RNA (ceRNA) hypothesis (9), lncRNAs interact with miRNAs through multiple mechanisms. These mechanisms include sponging of miRNAs by lncRNAs, competition for mRNA binding, and direct targeting of miRNAs by lncRNAs. Among these interactions, sponging is one of the most effective ways to regulate miRNAs (10). In various malignancies, dysregulated lncRNA expression contributes to tumor development, with individual lncRNAs acting as either oncogenic or tumor-suppressive regulators (11).

Dysregulated expression of lncRNAs has also been reported in the initiation and progression of EC, highlighting their importance as biomarkers and therapeutic targets (12). Upregulated lncRNA expression in malignant tissues correlates with increased tumor aggressiveness, driven by altered cell cycle control and reduced apoptosis (13). UCA1, classified as a lncRNA, acts as a ceRNA by interacting with miR-204, which prevents the downregulation of SOX4 and contributes to enhanced invasive and metastatic behavior in esophageal tumor cells (14).

Tumor suppressor lncRNAs inhibit cancer progression by suppressing cell proliferation and migration while promoting apoptosis. The lncRNA ADAMTS9-AS2, transcribed antisense to the tumor suppressor ADAMTS9, suppresses CDH3 expression in EC through epigenetic modulation of CpG island methylation, leading to reduced tumor cell functionality (15). Despite these studies, the role of lncRNAs in EC is not thoroughly characterized, and further research is needed to identify emerging lncRNAs in EC development.

This research aimed to discover novel lncRNAs in EC using integrated bioinformatic and experimental approaches. By analyzing EC data from The Cancer Genome Atlas (TCGA) database, we sought to identify candidate lncRNAs and their potential downstream genes, such as miRNAs and mRNAs, that might participate in EC pathogenesis. Following the bioinformatic analysis, we designed and conducted experimental assays to validate these computationally derived hypotheses.

## Methods

### TCGA data preprocessing

Esophageal cancer-related RNA and miRNA sequencing data, along with patient metadata, were sourced from the TCGA-ESCA project available on the GDC platform (<https://portal.gdc.cancer.gov/>). After excluding repeated samples, 184 samples with EC and 13 samples of tumor margin tissue were analyzed for all three categories of lncRNAs, miRNAs, and mRNAs.

Raw count matrices were filtered to remove low-abundance transcripts, followed by normalization using the GDCRNAtools pipeline to ensure comparability across samples. Batch effects were corrected when necessary, and sample integrity was verified through metadata cross-checking (Figure 1).

### Collection of samples from patients with EC

A total of 20 matched EC tissues and corresponding adjacent normal margins were obtained from the Iran National Tumor Bank, Tehran, Iran.

All specimens were histologically verified by a certified pathologist. Patients who had undergone chemotherapy, radiotherapy, or presented with recurrent tumors were excluded from the study.

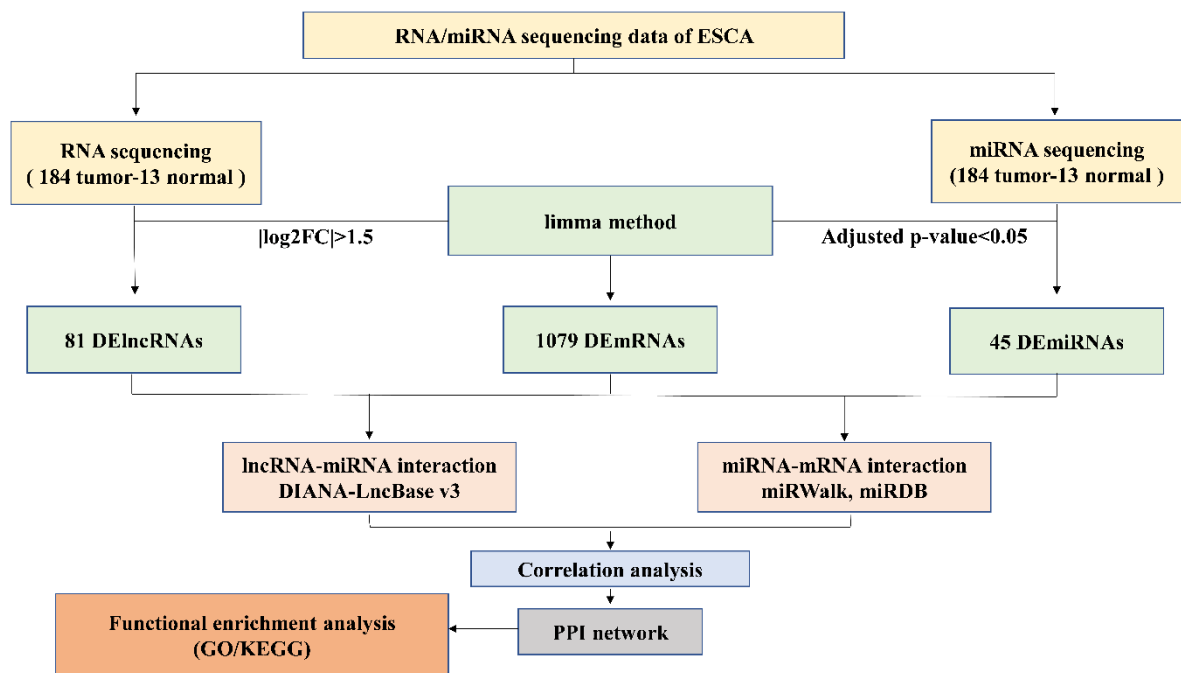


**Figure 1.** A flowchart demonstrating the bioinformatics methods applied in this research to discover the final regulatory axes for EC.

### Analysis of Differentially Expressed Genes (DEGs) in EC

The raw data downloaded from the TCGA database were preprocessed and normalized using GDCRNATools in R (V 4.3.2) as the initial analytical step. Differentially expressed lncRNAs, miRNAs, and mRNAs were identified using the limma package, applying thresholds of  $|\log_2 FC| \geq 1.5$  and adjusted  $p$ -value  $< 0.05$  (16). lncRNA-miRNA interaction predictions were conducted using the DIANA-LncBase v3 web tool, accessible at <https://diana.e-ce.uth.gr/lncbasev3>. Then, common miRNAs were obtained between those analyzed from the TCGA-ESCA and those predicted from DIANA-LncBase to determine each lncRNA target miRNA(s). miRNA-mRNA interactions were inferred by comparing predictions from miRWalk and miRDB.

### PPI network and Functional enrichment analysis

Using the StringApp plugin in Cytoscape version 3.10.3, a protein-protein interaction network was constructed, revealing 20 proteins linked to the target mRNAs of differentially expressed lncRNAs. To explore the biological pathways and functional enrichment of mRNAs, Gene Ontology (GO) and Kyoto Encyclopedia of Genes and Genomes (KEGG)

analyses were conducted using the clusterProfiler package in R. Statistical significance of the identified genes was confirmed based on  $p$  values less than 0.05.

### RT-qPCR Analysis

Total RNA was extracted from EC tissues and adjacent margin samples using RNX Plus reagent (Sinaclone, Iran).

Then, the purity and integrity of extracted RNA were confirmed using Nanodrop (Thermo Fisher Scientific Inc., USA) and 1% agarose gel. Furthermore, to ensure the absence of DNA contamination in the extracted RNA, we performed No RT (no reverse transcriptase) control reactions and verified that there was no amplification. cDNA was synthesized from one  $\mu\text{g}$  of RNA using a cDNA synthesis kit.

Targeted reverse transcription for RNU6 and hsa-miR-7-5p was performed using gene-specific primers (YT4500; Yektatajhez, Iran). The Roche Light Cycler 96 System was used to measure the relative expression levels of the selected target genes (Roche Life Science, Germany), employing RealQ Plus 2x Master Mix Green (Ampliqon, Denmark) for real-time PCR amplification. Expression levels were normalized using  $\beta$ -actin for mRNA targets and U6 small nuclear

RNA for miRNA quantification. The primer sequences used in this study are listed in Table 1.

#### Western blotting

Tissue samples were lysed using RIPA buffer containing a protease inhibitor cocktail obtained from

Kiazist, Iran. Protein concentration was measured using the BCA assay kit provided by DNAbiotech, Iran.

Following separation by SDS PAGE, proteins were transferred onto nitrocellulose membranes and blocked with five percent nonfat milk.

**Table 1. The primer sequences utilized in RT-qPCR.**

Primer sequence (5' to 3')		
<b>LINC02381</b>	Forward	AGACTGCCTGCCTAGAACA
	Reverse	AAGAACCCAAAGACGGAAG
<b>LINC00472</b>	Forward	ACCTCCTCTCCAACCTCACAGTA
	Reverse	TAAAGCAGCACACCCAAGTCTC
<b>FHIT</b>	Forward	ACTACAGCCAGGTAGCAGAAA
	Reverse	GCATGTGGTCAGATGGTAAAG
<b>β-actin</b>	Forward	CATGTACGTTGCTATCCAGGC
	Reverse	CTCCTTAATGTCACGCACGAT
<b>hsa-miR-7-5p</b>	Forward	CACGCTGGAAGACTAGTGATT
	Reverse	GCGTATCCAGTGCAGGGT
	stem-loop	GCGTATCCAGTGCAGGGTCCGAGGTATTCGCACTGGATAACGCAACAAC
<b>RNU6</b>	Forward	GCAAGGATGACACGCAAATTC
	Reverse	GCGTATCCAGTGCAGGGT
	stem-loop	GCGTATCCAGTGCAGGGTCCGATTCGCACTGGATAACGCAAAATATGGA

Membranes were incubated with primary antibodies targeting β-actin (sc-47778) and FHIT (sc-390481) for 24 hours at 4°C, then with HRP-conjugated secondary antibodies for 1 hour at room temperature. After thorough washing, protein bands were visualized using ECL advanced reagents. Protein band intensities were quantified in ImageJ (v1.41) by measuring the integrated density of each band after background subtraction. FHIT protein levels were normalized to β-actin by calculating the FHIT/β-actin ratio for each sample. Differences in FHIT protein expression between groups were calculated using the fold-change method and statistical comparisons were conducted using unpaired t- tests.

#### Immunohistochemistry (IHC)

Tissue fixation was performed with four percent formalin, followed by paraffin embedding to prepare blocks. Sections of five micrometers were cut and deparaffinized in xylene. FHIT primary antibody was applied for immunohistochemical staining (sc-

390481), followed by HRP-labeled streptavidin and a biotinylated anti-mouse secondary antibody kit (ab64264). Microscopic imaging was conducted at ×200 magnification using the BM-600 LED EPI fluorescent microscope. The density of the target protein FHIT in tumor samples was quantified using ImageJ software (v1.41). The obtained values were normalized by dividing each measurement by the mean FHIT density observed in the control group, and the normalized results were subsequently reported.

#### Statistical analysis

Statistical analyses were conducted using GraphPad Prism version 8 and SPSS version 26 software. Results are expressed as mean ± SEM, and differences were deemed statistically significant at a threshold of p-value < 0.05. Group comparisons and correlations were analyzed with t- test and Pearson's test for normally distributed data, or Mann-Whitney U and Spearman's test for non-normal data. Receiver operating characteristic (ROC) curves were generated

to evaluate the diagnostic potential of the selected genes in EC.

## Results

### Determination of DElncRNAs, DEmiRNAs, and DEMRNAs

Differentially expressed genes between EC tissues and adjacent margins were identified, revealing 81 DElncRNAs, 45 DEmiRNAs, and 1,079 DEMRNAs.

Among the DElncRNAs, those not investigated in previous EC studies were prioritized for further analysis (Figure 2).

### Prediction of lncRNA-miRNA-mRNA interactions

According to the ceRNA theory, lncRNAs regulate the expression of their target miRNAs. Similarly, miRNAs can regulate the expression of their target mRNAs.

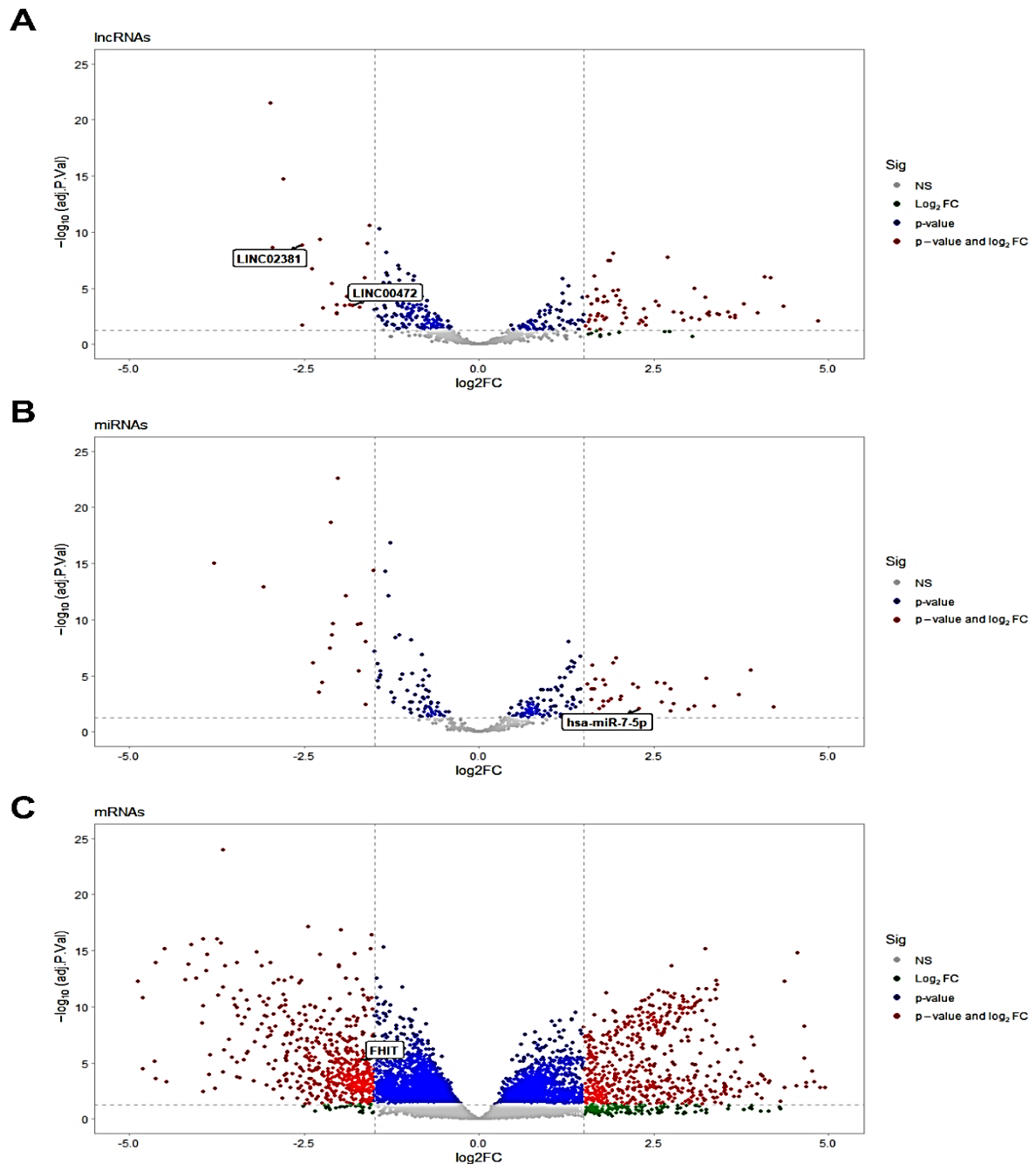


**Figure 2.** The volcano plot displays differentially expressed (DE) (A) lncRNAs, (B) miRNAs, and (C) mRNAs. Gray dots represent genes that did not meet either threshold ( $|\log_2\text{FC}| \geq 1.5$  or adjusted  $p < 0.05$ ). Green dots indicate genes with  $|\log_2\text{FC}| \geq 1.5$  but without statistical significance (adjusted  $p \geq 0.05$ ). Blue dots represent

**genes that were statistically significant (adjusted  $p < 0.05$ ) but had  $|\log_2 \text{FC}| < 1.5$ . Red dots highlight genes that met both criteria ( $|\log_2 \text{FC}| \geq 1.5$  and adjusted  $p < 0.05$ ).**

To identify miRNAs associated with up-regulated DElncRNAs, an intersection between the DIANA-LncBase v3 predicted miRNAs and down-regulated DEmiRNAs obtained from the TCGA-ESCA analysis was conducted.

Also, to identify the target miRNAs of down-regulated DElncRNAs, an intersection between the DIANA-LncBase v3 predicted miRNAs and up-regulated DEmiRNAs obtained from the TCGA-ESCA analysis was conducted.

miRNAs can cause degradation and non-translation of their target mRNAs. The commonality between their target mRNAs in miRWalk, miRDB, and mRNAs with high expression in TCGA-ESCA analysis was obtained to determine the target of miRNAs with low expression. Conversely, to determine the target of highly expressed miRNAs,

the commonality between their target mRNAs in miRWalk, miRDB, and mRNAs found to be low expressed in TCGA-ESCA analysis was obtained. Finally, after analyzing the DElncRNAs and identifying downstream miRNAs and mRNAs, LINC00472 and LINC02381 were selected. These lncRNAs were selected because of their novelty, the absence of prior studies in EC, and their established significance in other cancer types, as indicated by previous research. Additionally, their interactions with common miRNAs further supported their relevance.

Among these miRNAs, hsa-miR-7-5p exhibited a higher  $\log_2 \text{FC}$  compared to other candidates that met our selection criteria, making it particularly compelling for further investigation.

We also evaluated downstream molecules of hsa-miR-7-5p using bioinformatic tools, and FHIT was selected due to exhibiting the most substantial negative  $\log_2 \text{FC}$  among the identified candidates. As a result, the LINC00472/hsa-miR-7-5p/FHIT and LINC02381/hsa-miR-7-5p/FHIT axes were obtained based on bioinformatic analysis.

### Correlation analysis

Significant positive correlations were observed between LINC00472 and FHIT, LINC02381 and FHIT ( $p\text{-value} < 0.05$ ). Box plots display expression of genes in TCGA-ESCA data, showing downregulated

LINC00472, LINC02381, FHIT, and upregulated hsa-miR-7-5p in EC (Figure 3).

### PPI analysis of FHIT

A protein interaction network centered on FHIT revealed several key partners, including TP53, DAPK1, and MDM2. These interacting proteins form a closely connected cluster involved in the regulation of cellular apoptosis, underscoring the central role of FHIT within this functional network (Figure 4).

### GO and KEGG analysis

Within the biological process (BP) category of GO, the most significantly enriched term was the intrinsic apoptotic signaling pathway by p53 class mediator (Figure 5A). Also, the top result in the cellular component (CC) is the transcription repressor complex (Figure 5B). In addition, in molecular function (MF), these genes are involved in hydrolase activity, acting on carbon-nitrogen (Figure 5C). In the KEGG, FHIT-related genes were predominantly involved in Bladder cancer (Figure 5D).

### Expression and Correlation Analysis of LINC00472, LINC02381, hsa-miR-7-5p, and FHIT in EC

RT-qPCR quantified the expression levels of LINC02381, LINC00472, hsa-miR-7-5p, and FHIT in EC tissues and adjacent margins. LINC02381 ( $p\text{-value} < 0.001$ ) and LINC00472 ( $p\text{-value} < 0.0001$ ) were significantly downregulated in EC. Conversely, hsa-miR-7-5p was upregulated in EC ( $p\text{-value} < 0.0001$ ). FHIT showed marked downregulation at both mRNA and protein levels (Figure 6), corroborated by IHC ( $p\text{-value} < 0.01$ ) (Figure 7). Furthermore, correlations among the studied genes were evaluated in EC patients.

A statistically significant positive correlation was observed between LINC02381 and FHIT expression levels ( $p\text{-value} < 0.05$ ). In contrast, although LINC00472 expression showed a positive trend with FHIT expression, this association did not reach statistical significance ( $p\text{-value} > 0.05$ ). Both lncRNAs genes correlated negatively with hsa-miR-7-5p but FHIT and hsa-miR-7-5p correlation was non-significant (Figure 6).

### Clinicopathological features of patients with EC

This study included 20 individuals diagnosed with EC, of whom 60% were females and 40% males. The mean age of participants was 65.7 years, accompanied by a standard deviation of 11.56 years. In addition, among the 20 EC samples analyzed, 17 were esophageal squamous cell carcinoma (ESCC) and three were esophageal adenocarcinoma (EAC). A chi-square test was employed to evaluate the association between gene expression and clinical pathology data. As a result, hsa-miR-7-5p correlated with muscularis propria involvement and vascular invasion ( $p$ -

value<0.05), while FHIT expression was linked to necrosis and vascular invasion ( $p$ -value<0.05). In contrast, LINC02381 and LINC00472 showed no significant clinical associations ( $p$ -value>0.05). These results suggest hsa-miR-7-5p and FHIT play key roles in EC progression, whereas LINC02381 and LINC00472 may act indirectly via regulation of these genes, supporting the ceRNA hypothesis. Given the limited number of samples within the clinical subgroups, the clinicopathological associations are interpreted within the context of this cohort

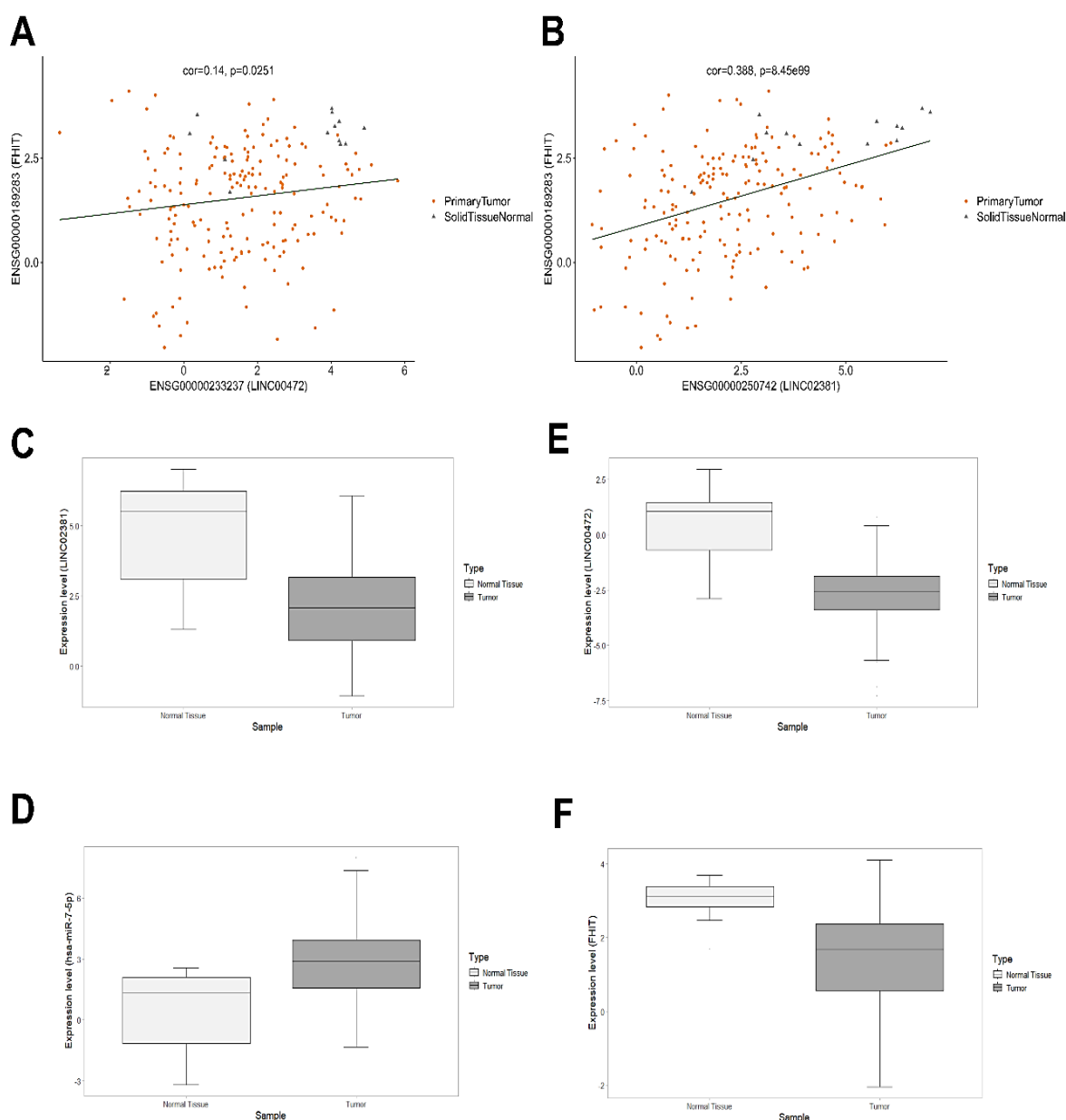


**Figure 3. Correlation analysis and genes expression (n=197). (A) Correlation between LINC00472 and FHIT with Pearson's Test. (B) Correlation between LINC02381 and FHIT with Pearson's Test. (C-D) Decreased**

LINC02381 and LINC00472 expression in EC samples relative to tumor margins, (E) Elevated hsa-miR-7-5p gene expression in EC samples, and (f) Decreased expression of FHIT in EC as a tumor suppressor.

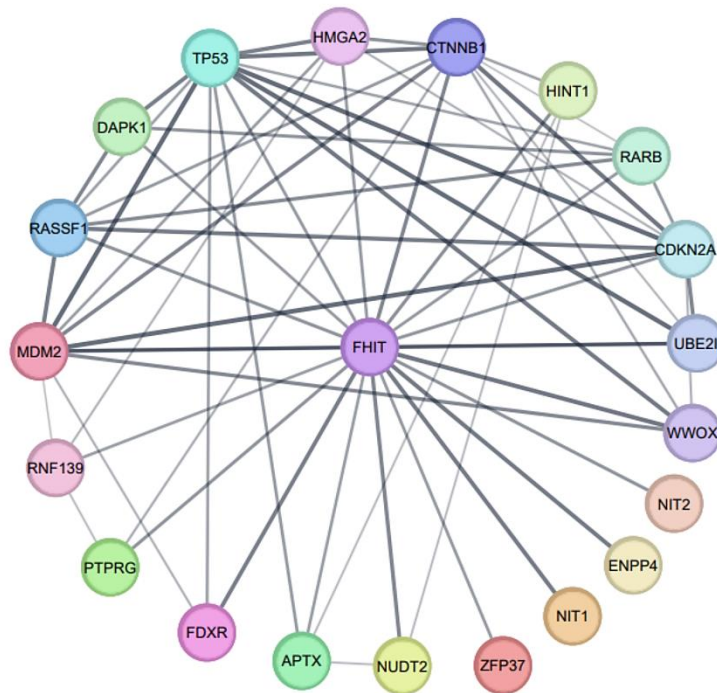


Figure 4. The PPI network of FHIT was constructed using the StringApp plugin within Cytoscape software.

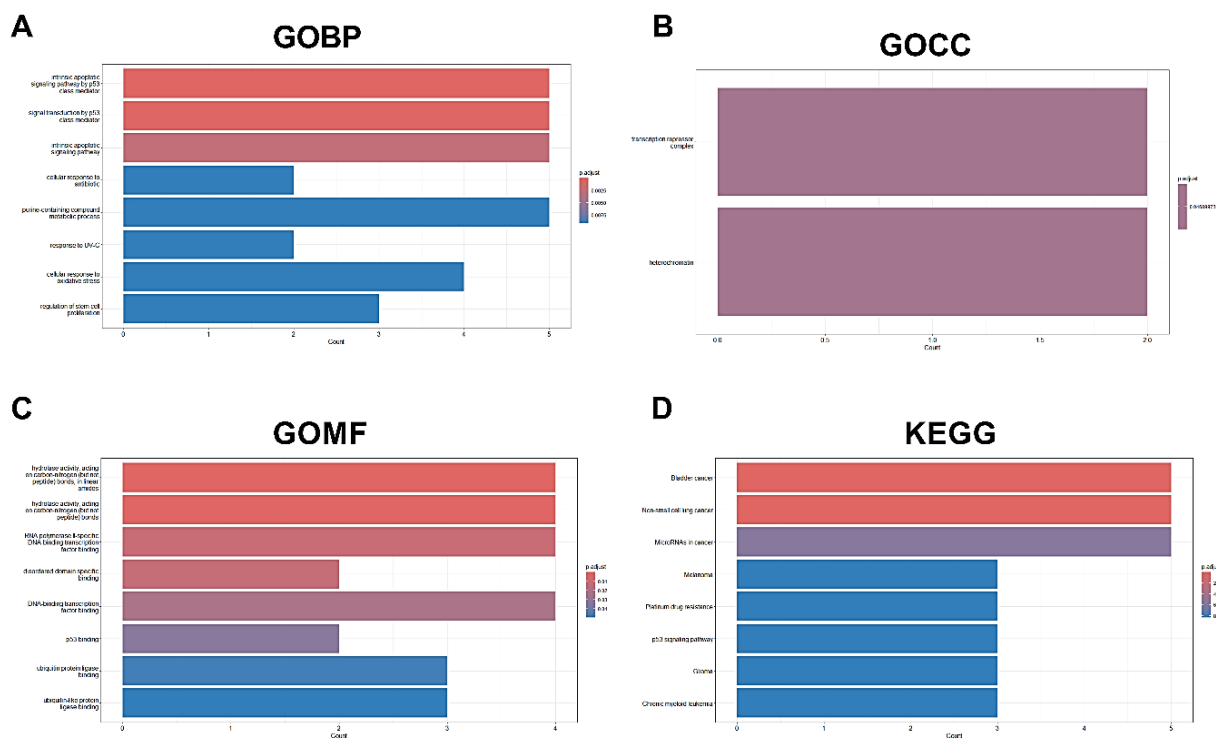
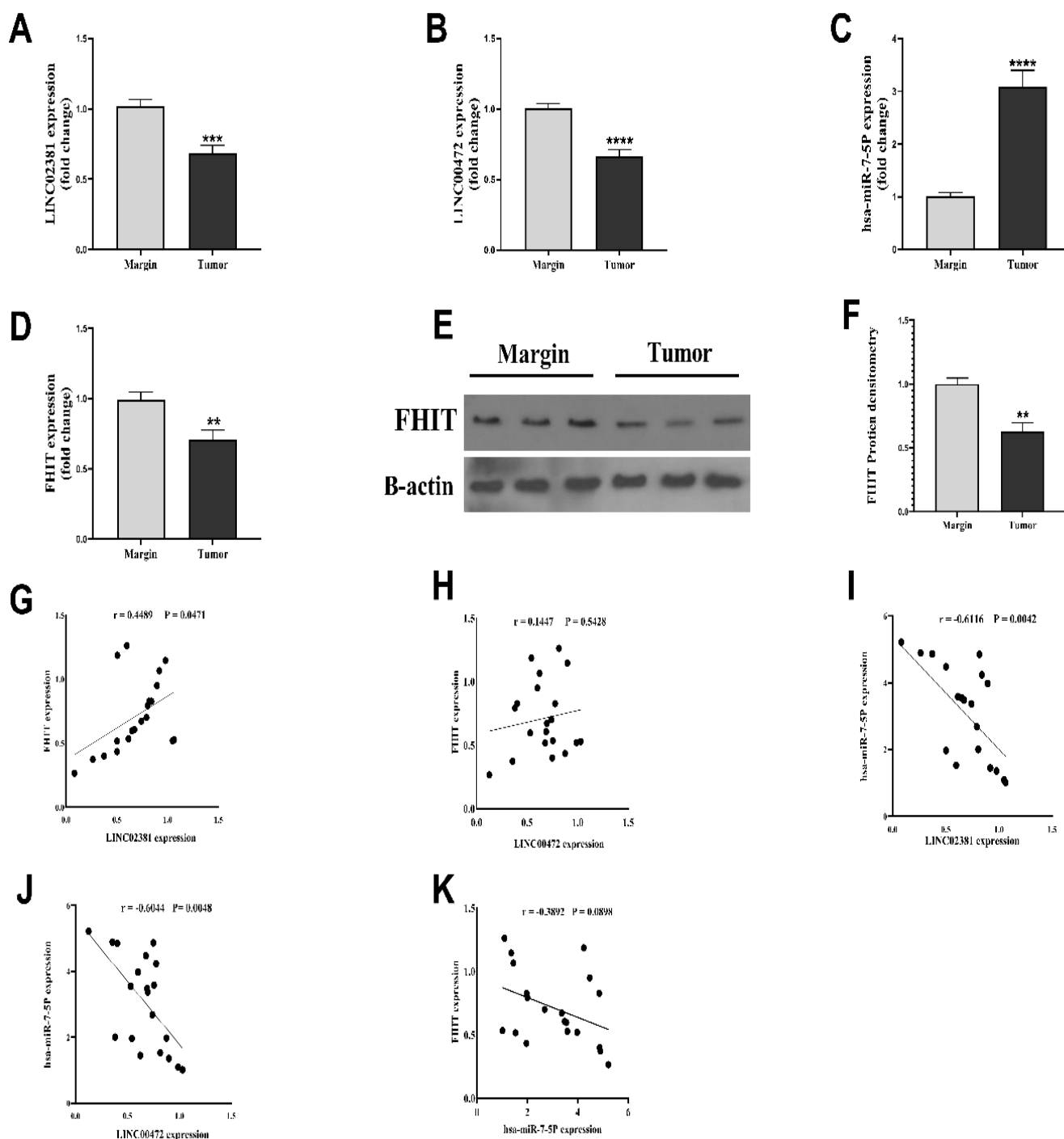


Figure 5. Bar plots illustrating Gene Ontology (GO) and Kyoto Encyclopedia of Genes and Genomes (KEGG) enrichment analyses were produced using the clusterProfiler package in R. These visualizations highlight

[ DOI: 10.22088/IJMC.M.BUMS.15.1.1143 ] [ Downloaded from ijmcmed.org on 2026-05-27 ]

significantly enriched terms across GO categories, including (A) biological process (BP), (B) cellular component (CC), and (C) molecular function (MF), as well as (D) enriched pathways identified through KEGG analysis.



**Figure 6.** Examination of genes expression in patients with EC (n = 20) and correlation between them. (A) LINC02381 expression, (B) LINC00472 expression, (C) hsa-miR-7-5p expression, (D) FHIT expression in EC tissue. (E-F) FHIT protein levels were assessed via Western blotting, with quantification presented as mean  $\pm$  SEM following normalization to  $\beta$ -actin. (G) Correlation analysis between LINC02381 and FHIT, (H) Correlation analysis between LINC00472 and FHIT, (I) Correlation analysis between LINC02381 and hsa-miR-7-5p, (J) Correlation analysis between LINC00472 and hsa-miR-7-5p. (K) Correlation analysis between

**FHIT and hsa-miR-7-5p genes expression.  $p < 0.01$  (\*\*),  $p < 0.001$  (\*\*\*),  $p < 0.0001$  (\*\*\*\*). Statistical significance was assessed using unpaired t- tests for expression comparisons (A–F) and Pearson correlation analysis for panels (G–K).**

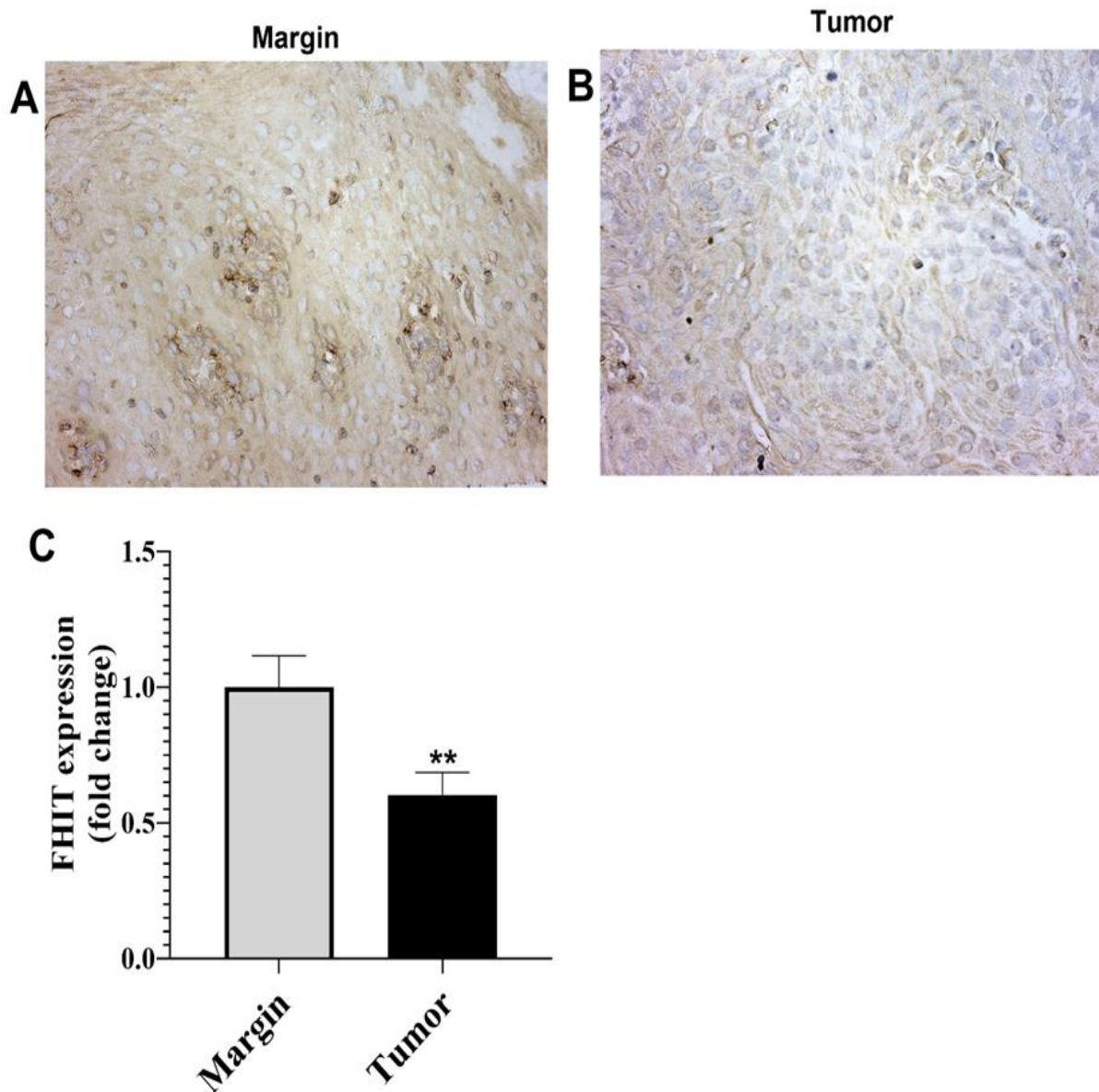


**Figure 7. Selected images from IHC staining of FHIT. (A) Tumor margin tissue at x200 magnification, (B) Tumor tissue at x 200 magnification. C FHIT protein expression in EC tumors is significantly reduced compared to tumor margins (\*\* $p < 0.01$ ). Statistical significance was assessed using Mann–Whitney U test for expression comparisons.**

#### ROC curve analysis

ROC curve analysis was conducted using  $2^{-\Delta Ct}$  values to assess the diagnostic potential of LINC02381, LINC00472, hsa-miR-7-5p, and FHIT in distinguishing EC tissues from tumor margins. The

AUCs were 0.73 (LINC02381), 0.8 (LINC00472), 0.72 (hsa-miR-7-5p), and 0.75 (FHIT), indicating moderate to strong diagnostic accuracy. For each gene, the corresponding values of specificity,

sensitivity, and confidence intervals are presented in the respective figure.

These findings suggest that all four genes, particularly LINC00472, may serve as effective biomarkers for EC detection (Figure 8).

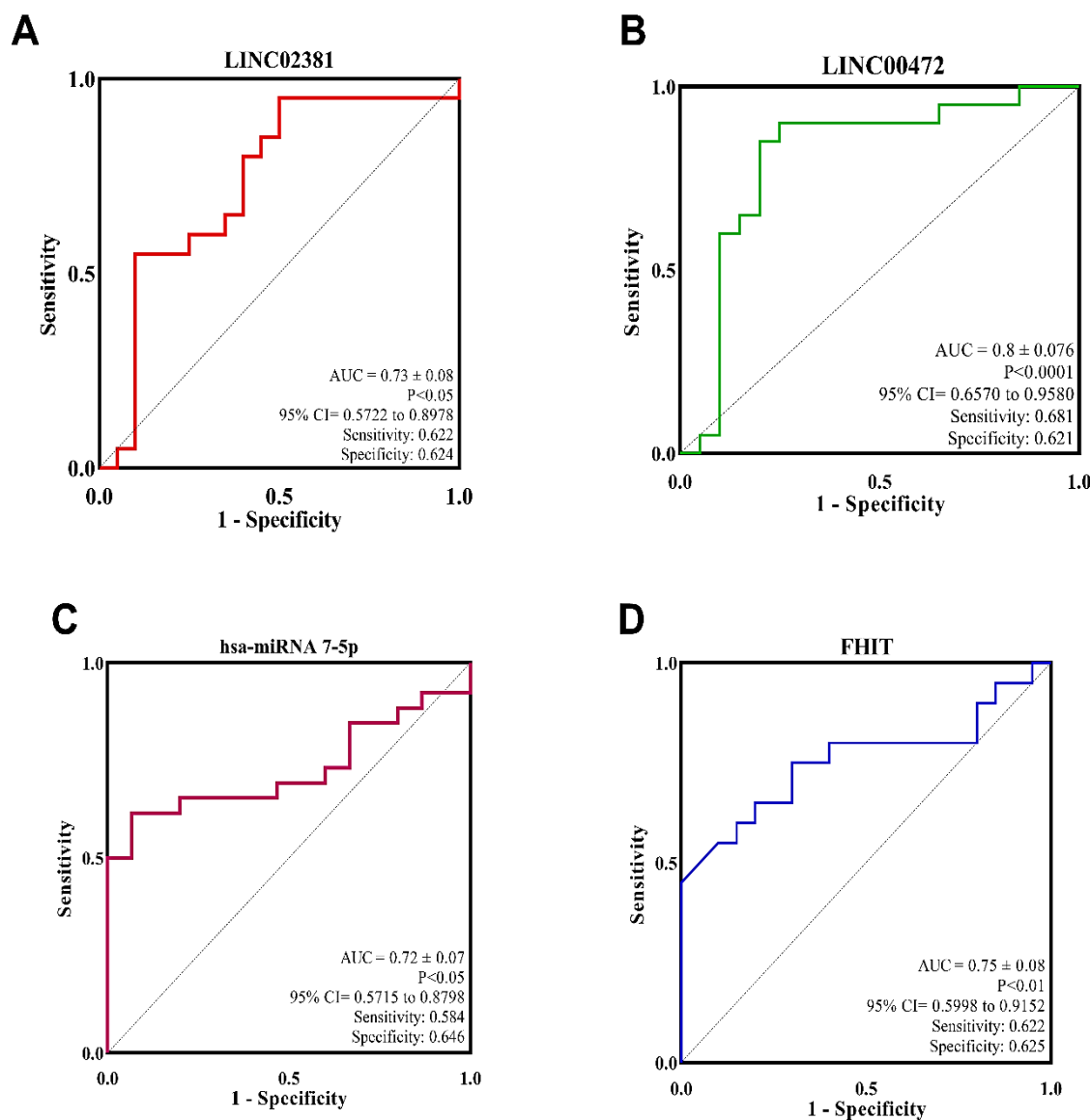


**Figure 8.** ROC curves were generated to assess the diagnostic accuracy of LINC02381, LINC00472, hsa-miR-7-5p, FHIT, and their combined panel in distinguishing EC tumor tissues (n = 20).

## Discussion

EC is a disease with a low survival rate in affected individuals. Current primary treatments for EC include surgery, radiotherapy, and chemotherapy, which are not satisfactory due to limited efficacy and severe side effects (17). Targeted therapy of genes and other components effective in EC, such as EGFR and VEGF, is growing as a new type of treatment in patients with this cancer (18). As a new biomarker,

lncRNAs can help diagnose EC earlier, improve treatment effectiveness, and increase patients' survival rates. lncRNAs can also be used as a target for targeted therapy methods (19).

Oncogenic lncRNAs promote tumor progression by sponging tumor-suppressive miRNAs, whereas tumor-suppressor lncRNAs exert opposing effects by sponging oncogenic miRNAs (4). Based on integrated bioinformatic analyses and experimental expression

profiling, this study suggests that LINC00472, LINC02381, and FHIT may act as tumor-suppressor-associated genes in EC, while hsa-miR-7-5p may exhibit oncogenic features. However, the proposed regulatory relationships are inferred from correlative evidence and require functional validation. To the best of our knowledge, the predicted interactions between LINC00472, LINC02381 and hsa-miR-7-5p have not been previously reported in EC, highlighting the novelty of the proposed regulatory axes.

LINC00472 is located on chromosome 6q13 and has four exons. The LINC00472 expression pattern has been reported in various types of cancers (20), acute liver damage (21), and primary bile cholangitis (22). In alignment with our results, previous studies have identified LINC00472 as a tumor suppressor in various malignancies, underscoring its potential role in inhibiting cancer progression.

Previous studies have shown that LINC00472 can sponge oncogenic miRNAs such as miR-4311 (20) and miR-23A-3p (23). Likewise, LINC00472 can regulate oncogenic signaling pathways, such as MEK/ERK, by inducing epigenetic modifications that suppress MCM6 expression, thereby contributing to tumor suppression (24).

While LINC00472 appears to act predominantly as a tumor suppressor in several malignancies, studies on LINC02381 are more contradictory. In some cancers, including cervical cancer (25), it plays an oncogenic role, but in breast cancer, LINC02381 has also been identified as a tumor suppressor, consistent with our findings (26).

In cervical cancer, LINC02381, by sponge miR-590-5p and miR-133b, increases cell migration and further survival of cancer cells (27). Conversely, LINC02381 has been shown to regulate the PI3K signaling pathway and exert notable tumor-suppressive effects in colorectal cancer through modulation of this pathway (28).

Based on our bioinformatic analyses, LINC00472 and LINC02381 are predicted to interact with hsa-miR-7-5p. hsa-miR-7-5p plays a role in gene expression and post-transcriptional modulation in humans and other species (29). hsa-miR-7-5p expression across different cancer types have yielded inconsistent findings in the literature.

Recent investigations have highlighted the tumor-suppressive function of hsa-miR-7-5p across various

malignancies, including lymphoma, gastric carcinoma, and glioma (30). However, consistent with the results of our study, the expression of hsa-miR-7-5p significantly increased in small intestinal endocrine neoplasia (31). We determined that expression of hsa-miR-7-5p in EC is associated with muscularis propria involvement and vascular invasion levels. hsa-miR-7-5p influences key cellular processes, including metastasis and cell proliferation, through the regulation of its downstream target genes. On the other hand, increased muscularis propria leads to increased tumor ability to invade surrounding tissues (32). Consistent with our integrative analysis, hsa-miR-7-5p is also predicted to target the Fragile histidine triad (FHIT) gene, a well-known tumor suppressor.

FHIT belongs to the histidine triad (HIT) family of hydrolyzing proteins and is widely recognized for its tumor-suppressive properties. Aberrant downregulation of FHIT expression has been documented in various cancers, such as gastric, renal, cervical, lung, and head and neck carcinomas (33). In lung cancer, the FHIT protein induces apoptosis by inducing the Fas cell surface death receptor, caspase 8, and on the other hand, it maintains apoptotic function by increasing cytochrome c from mitochondria (34). In our study, FHIT expression at both gene and protein levels significantly decreased in EC tissues compared to tumor margin tissues. Our findings indicate that hsa-miR-7-5p may contribute to FHIT downregulation; however, promoter hypermethylation has also been reported as a mechanism leading to FHIT suppression in EC (35). Functional enrichment analysis also revealed that FHIT and proteins that interact with it are more involved in cell death and apoptosis pathways. Increased FHIT expression increased necrosis in patients with EC in our study. FHIT has been demonstrated to promote apoptosis and cell cycle arrest, thereby suppressing tumor cell proliferation. Additionally, FHIT influences tumor-associated inflammatory responses and may activate necrotic cell death pathways (36, 37).

This study also associated increased FHIT expression with decreased vascular invasion. Consistent with these findings, loss of heterozygosity at the FHIT locus in gastric cancer has been associated with pathological primary tumors, regional lymph node involvement, and vascular invasion (38). These

clinicopathological correlations should be considered preliminary and require validation in larger, more balanced cohorts.

The interactions among LINC00472, LINC02381, hsa-miR-7-5p, and FHIT have not yet been fully characterized. In our cohort, a statistically significant positive correlation was identified between LINC02381 and FHIT expression, whereas LINC00472 exhibited a positive but non-significant trend with FHIT.

Furthermore, a negative correlation was observed between hsa-miR-7-5p and both LINC02381 and LINC00472, supporting the notion of a potential ceRNA-like regulatory relationship. The ROC curves for LINC00472, LINC02381, hsa-miR-7-5p, and FHIT demonstrated notable AUC values, suggesting their potential relevance as diagnostic indicators in EC. Among these, LINC00472 showed the highest AUC value and the lowest p-value. While these results highlight possible biomarker roles, further validation is required before considering their clinical utility or therapeutic implication.

This study demonstrated a significant downregulation of LINC00472 and LINC02381 expression in EC. Furthermore, we examined potential downstream genes of these lncRNAs and identified hsa-miR-7-5p and FHIT as likely candidates. Given these observations, and while our experimental validation utilized 20 paired EC, future studies with larger cohorts would provide additional confirmation of these expression patterns and strengthen the statistical robustness of the observed associations.

Additionally, investigations incorporating blood samples from EC patients, with separate examinations of the two subtypes ESCC and EAC, could further validate the clinical utility of these biomarkers. In addition, mechanistic experiments such as luciferase reporter assays will be essential for verifying the regulatory interactions within these axes. Functional studies, including gene knockdown or overexpression, will also be valuable in clarifying how these axes contribute to cancer development.

This study demonstrates expression patterns of LINC00472, LINC02381, hsa-miR-7-5p, and FHIT in EC and proposes a putative ceRNA network based on bioinformatic predictions and correlative expression analyses. The downregulation of LINC00472 and

LINC02381, alongside the upregulation of hsa-miR-7-5p in EC, supports their involvement in a ceRNA network. FHIT expression was also reduced in EC at both mRNA and protein expression. ROC analysis suggested diagnostic potential, particularly for LINC00472.

Statistically significant associations were found between hsa-miR-7-5p and muscularis propria involvement, as well as between FHIT expression and necrosis and reduced vascular invasion. These findings suggest that these genes may serve as promising exploratory biomarkers and potential therapeutic targets in EC and provide a foundation for future functional investigations.

In particular, mechanistic studies aimed at validating the hypothesized ceRNA interactions among LINC00472, LINC02381, hsa-miR-7-5p, and FHIT are warranted to clarify their precise roles in EC pathogenesis.

## Acknowledgments

We would like to thank the Department of Clinical Biochemistry of Hamadan University of Medical Sciences for their invaluable support throughout present study.

## Funding

The study was funded by the Vice-Chancellor for Research and Technology, Hamadan University of Medical Sciences (No. 140305164030).

This research received ethical approval from the Ethics Committee of Hamadan University of Medical Sciences (Ethical Code: IR.UMSHA.REC.1403.292) and was conducted in full compliance with the principles outlined in the Declaration of Helsinki. Informed consent was obtained from all participants, their privacy and confidentiality were rigorously protected.

## References

1. Younesian O, Sheikh Arabi M, Jafari SM, et al. Long-Term Excessive Selenium Supplementation Affects Gene Expression in Esophageal Tissue of Rats. *BBiol. Trace Elem. Res.* 2023;201(7):3387-94.

2. Sabri S, Mahani SE, Al-Shammari AM, et al. Lactobacillus Plantarum and its Derived Bacteriocin Exhibits Potent Antitumor Activity against Esophageal Cancer Cells. *Int. J. Mol. Med.* 2024;13(3):286-302.
3. Zeng H, Chen W, Zheng R, et al. Changing cancer survival in China during 2003-15: a pooled analysis of 17 population-based cancer registries. *Lancet Glob Health.* 2018;6(5):e555-e67.
4. Nemeth K, Bayraktar R, Ferracin M, et al. Non-coding RNAs in disease: from mechanisms to therapeutics. *Nat. Rev. Genet.* 2024;25(3):211-32.
5. Bahmani M, Kalantary-Charvadeh A, Hamrahjoo M, et al. Expression patterns, regulatory interactions, and diagnostic potential of LINC00839 and LINC01605 in esophageal cancer. *Biochem. Biophys. Res. Commun.* 2025;44:102305.
6. Chen L-L, Kim VN. Small and long non-coding RNAs: Past, present, and future. *Cell.* 2024;187(23):6451-85.
7. Uppaluri KR, Challa HJ, Gaur A, et al. Unlocking the potential of non-coding RNAs in cancer research and therapy. *Transl Oncol.* 2023;35:101730.
8. Bridges MC, Daulagala AC, Kourtidis A. LNCcation: lncRNA localization and function. *J Cell Biol.* 2021;220(2).
9. Ala U. Competing Endogenous RNAs, Non-Coding RNAs and Diseases: An Intertwined Story. *Cells.* 2020;9(7).
10. Ma B, Wang S, Wu W, et al. Mechanisms of circRNA/lncRNA-miRNA interactions and applications in disease and drug research. *Biomed. Pharmacother.* 2023;162:114672.
11. Kalantary-Charvadeh A, Morovat S, Aslani S, et al. The role of long non-coding RNA LINC00839 in oral squamous cell carcinoma based on bioinformatics and experimental research. *Sci Rep.* 2024;14(1):31817.
12. Yang C, Chen K. Long Non-Coding RNA in Esophageal Cancer: A Review of Research Progress. *Pathol Oncol Res.* 2022;28:1610140.
13. Qi Y, Song C, Zhang J, et al. Oncogenic lncRNA CASC9 in Cancer Progression. *Curr Pharm Des.* 2021;27(4):575-82.
14. Jiao C, Song Z, Chen J, et al. lncRNA-UCA1 enhances cell proliferation through functioning as a ceRNA of Sox4 in esophageal cancer. *Oncol Rep.* 2016;36(5):2960-6.
15. Liu D, Wu K, Yang Y, et al. Long noncoding RNA ADAMTS9-AS2 suppresses the progression of esophageal cancer by mediating CDH3 promoter methylation. *Mol Carcinog.* 2020;59(1):32-44.
16. Marhamati S, Abbasalipourkabir R, Seyedkhan Z, et al. Investigating the expression of hsa\_circ\_0036722/hsa-miR-503-5p/PDCD4 axis in esophageal cancer. *Disc Oncol.* 2025.
17. Marhamati S, Hamrahjoo M, Seyedkhan Z, et al. KRT6A, KRT6B, PKP1, and PKP3 as key hub genes in esophageal cancer: A combined bioinformatics and experimental study. *Biochem. Biophys. Res. Commun.* 2025;43:102095.
18. Yang Y-M, Hong P, Xu WW, et al. Advances in targeted therapy for esophageal cancer. *Signal Transduct. Target. Ther.* 2020;5(1):229.
19. Wang W, Ye L, Li H, et al. Targeting esophageal carcinoma: molecular mechanisms and clinical studies. *MedComm (2020).* 2024;5(11):e782.
20. Zou C, Lv X, Wei H, et al. Long non-coding RNA LINC00472 inhibits oral squamous cell carcinoma via miR-4311/GNG7 axis. *Bioengineered.* 2022;13(3):6371-82.
21. Li L, He Y, He XJ, et al. Down-regulation of long noncoding RNA LINC00472 alleviates sepsis-induced acute hepatic injury by regulating miR-373-3p/TRIM8 axis. *Exp Mol Pathol.* 2020;117:104562.
22. Dong XH, Dai D, Yang ZD, et al. S100 calcium binding protein A6 and associated long noncoding ribonucleic acids as biomarkers in the diagnosis and staging of primary biliary cholangitis. *World J Gastroenterol.* 2021;27(17):1973-92.
23. Yang S, Liu Y, Li Y, et al. LINC00472 suppresses non-small cell lung cancer progression via regulating miR-23a-3p/CCL22 axis. *Cell Mol Biol.* 2024;70(6):54-60.
24. Shao G, Fan X, Zhang P, et al. Methylation-dependent MCM6 repression induced by LINC00472 inhibits triple-negative breast cancer metastasis by disturbing the MEK/ERK signaling pathway. *Aging.* 2021;13(4):4962-75.
25. Chen X, Zhang Z, Ma Y, et al. LINC02381 Promoted Cell Viability and Migration via Targeting miR-133b in Cervical Cancer Cells. *Cancer Manag Res.* 2020;12:3971-9.

26. Golestan S, Soltani BM, Jafarzadeh M, et al. LINC02381 suppresses cell proliferation and promotes apoptosis via attenuating IGF1R/PI3K/AKT signaling pathway in breast cancer. *Funct Integr Genomics*. 2023;23(1):40.
27. Wang J, Zhao Q. Linc02381 Exacerbates Rheumatoid Arthritis Through Adsorbing miR-590-5p and Activating the Mitogen-Activated Protein Kinase Signaling Pathway in Rheumatoid arthritis-fibroblast-like synoviocytes. *Cell Transplant*. 2020;29:963689720938023.
28. Jafarzadeh M, Soltani BM, Soleimani M, et al. Epigenetically silenced LINC02381 functions as a tumor suppressor by regulating PI3K-Akt signaling pathway. *Biochimie*. 2020;171-172:63-71.
29. Møller HG, Rasmussen AP, Andersen HH, et al. A systematic review of microRNA in glioblastoma multiforme: micro-modulators in the mesenchymal mode of migration and invasion. *Mol Neurobiol*. 2013;47(1):131-44.
30. Kalinowski FC, Brown RA, Ganda C, et al. microRNA-7: a tumor suppressor miRNA with therapeutic potential. *Int J Biochem Cell Biol*. 2014;54:312-7.
31. Heverhagen AE, Legrand N, Wagner V, et al. Overexpression of MicroRNA miR-7-5p Is a Potential Biomarker in Neuroendocrine Neoplasms of the Small Intestine. *Neuroendocrinology*. 2018;106(4):312-7.
32. He K, Chen C, Xia L, et al. Deep muscularis propria tumor invasion without lymph node metastasis as a unique subclassification of stage IB gastric cancer: a retrospective study. *BMC Gastroenterol*. 2022;22(1):30.
33. Huber O, Weiske J. Beta-catenin takes a HIT. *Cell Cycle*. 2008;7(10):1326-31.
34. Roz L, Andriani F, Ferreira CG, et al. The apoptotic pathway triggered by the Fhit protein in lung cancer cell lines is not affected by Bcl-2 or Bcl-x(L) overexpression. *Oncogene*. 2004;23(56):9102-10.
35. Hassan MI, Naiyer A, Ahmad F. Fragile histidine triad protein: structure, function, and its association with tumorigenesis. *J Cancer Res Clin Oncol*. 2010;136(3):333-50.
36. Sard L, Accornero P, Torielli S, et al. The tumor-suppressor gene FHIT is involved in the regulation of apoptosis and in cell cycle control. *Proc Natl Acad Sci U S A*. 1999;96(15):8489-92.
37. Deng W-G, Nishizaki M, Fang B, et al. Induction of apoptosis by tumor suppressor FHIT via death receptor signaling pathway in human lung cancer cells. *Biochem. Biophys. Res. Commun*. 2007;355(4):993-9.
38. Noguchi T, Müller W, Wirtz HC, et al. FHIT gene in gastric cancer: association with tumour progression and prognosis. *J Pathol*. 1999;188(4):378-81.